Active Digital Microfluidic Paper Chips with Inkjet-Printed Patterned Electrodes

Hyojin Ko, Jumi Lee, Yongjun Kim, Byeongno Lee, Chan-Hee Jung, Jae-Hak Choi, Oh-Sun Kwon, and Kwanwoo Shin**

By virtue of the abundance and physical properties of cellulose, paper-based devices are often considered to be novel platforms for inexpensive, portable, and simple devices.[1–4] These advantages have motivated the development of diverse paper-based applications, including biochemical,[5] mechanical,[6] and electrical applications.[2,7] Another unique characteristic of paper—its ability to permit precise writing and printing—has also been used to develop various novel devices,[8–14] such as patterned bioassays on paper,[9,12] inkjet-printed chemical-sensing paper,[11,13] and an electronic paper display.[14]

The first promising paper diagnostic chip was introduced by the Whiteside group in 2007,[15] and recently significant attention has been paid to paper-based fluidic devices.[1,5,8–14] Paper-based fluidic devices primarily offer the advantages of portability, absorbability, disposability, and significantly lower costs over conventional fluidic devices, which require meticulous fluidic controls with pumps and valves.[16] Most conventional paper chips commonly use a selective technique to convert from hydrophilic to hydrophobic paper or vice versa, and the flow of the sample through hydrophilic-patterned channels isolated by hydrophobic, waterproof walls is actuated by the competition between attractive and repulsive capillary forces.[5] These passive chips, therefore, have two principal limitations: a) transport of the liquid sample as a continuous flow is primarily by the capillary force of the cellulose fibers; and b) reactions occur at the terminals of the patterned array on which the chemical reagents have been pre-implanted or printed as detecting or diagnostic probes.

H. Ko, Prof. J. Lee, Y. Kim, Dr. B. Lee, Prof. O.-S. Kwon
Department of Chemistry and Institute of Biological Interfaces
Sogang University
Seoul 121–742, Republic of Korea
E-mail: oskwon@sogang.ac.kr

C.-H. Jung
Advanced Radiation Technology Institute
Korea Atomic Energy Research Institute
Jeongeup 580–185, Republic of Korea

Dr. J.-H. Choi
Department of Polymer Science and Engineering
Chungnam National University
Daejeon 305–764, Republic of Korea

Prof. K. Shin
Department of Chemistry and Institute of Biological Interfaces
Sogang University
Seoul 121–742, Republic of Korea
School of Engineering and Applied Science
Harvard University
Cambridge, MA 02138, USA
E-mail: kwshin@sogang.ac.kr

DOI: 10.1002/adma.201305014

Whereas previous research on paper microfluidic chips focused on fully integrated lab-on-a-chip (LOC) devices[16] and on manipulating a continuous fluid in two- or three-dimensional channels[7,17] by utilizing only the passive capillary force of the paper itself to reduce costs, no attempt has been made to manipulate electric drop actuation by using external power sources, presumably because of the complexities involved in implementing electric circuits on paper devices.[1,2,18,19] A surface-energy trap-based drop manipulation technique in which a magnetic field was manually varied to enable drop transport and fusion and to allow liquid to be dispensed was introduced recently; however, the absence of electric implementation has limited the programmable automated time-delay motion of the technique.[20]

In this study, we present a novel, paper-based fluidic chip that allows the full range of fluidic operations by implementing an electric input on paper via an electrowetting technique.[21–25] This powered paper-based microfluidic chip, which is known as an active paper open chip (APOC), is primarily characterized by discrete drop volumes and is an open-type chip.[26–28] The most noticeable difference between active and passive paper-based microfluidic devices is the existence of a patterned array of electrodes on the paper such that the capillary force on the substrate's surface can be actively tuned with an external voltage. The basic principle of actuating drops on paper is the use of an electric field to adjust the electrowetting-induced surface tension between a drop and a counter-electrode beneath the surface. Hence our APOC has unique advantages over the conventional passive transporting chips. Essentially, on our APOC, it is possible to perform diluting, merging and/or mixing of the sample drops, having pre-determined quantized volumes. Prior to the main reaction with a target drop, pre-programmed sequential treatments with various reagents at exact time can be readily accomplished, simplifying the workflow and improving the reaction accuracy tremendously in the laboratory to the conventional methods. These features surely allow the potential usages of the APOCs to be realized, often requiring multiple pre-treatments, such as sample preparations for matrix-assisted light deposition/ionization (MALDI) analysis[29] or enzyme-linked immunosorbent assay (ELISA).[15,30] Various open devices[28] have been developed following Washizu's demonstration[26] of an open digital microfluidic chip a decade ago; however, most devices still operate on rigid, solid substrates, such as glass,[27] silicon,[31] or polymers.[32] The key advantage in fabricating APOCs is that electrode patterns can be designed and printed on paper quickly, finely, and precisely without complicated wet-lab processes. A printing method could become the simplest all-in-one method for designing and printing, thereby replacing complex, multi-step conventional optical lithography and allowing chip production at the point

ADVANCED MATERIALS
www.advmat.de

www.MaterialsViews.com

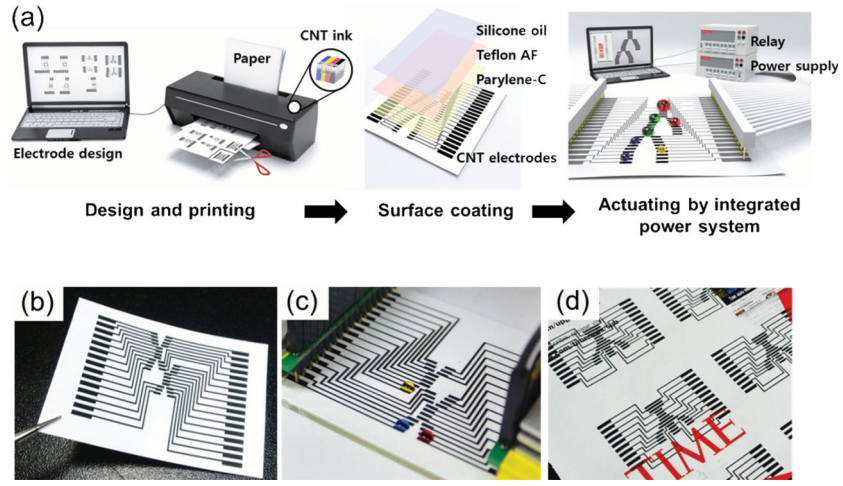

Figure 1. a) Overview of the fabrication process for an active microfluidic paper chip: design using a personal computer and inkjet-printing of the patterned electrodes; coating with dielectric and oil films; actuation of reagent drops on the paper chip by using an integrated switching power system. b) Photograph of the printed paper chip; c) photograph of a microfluidic paper chip assembled in the integrated switching power system; and d) photograph of the patterned electrodes on *Time* magazine paper to show their potential use with a cheap and ubiquitous recycled material (Time logo reproduced with permission from Time magazine).

of care, particularly in remote and isolated regions with limited resources.[9,10] To demonstrate the simplicity of this production process, we used inkjet printing with a commercial home or office inkjet printer and fabricated electrodes on commercially available photo paper by using a homemade conductive ink of carbon nanotubes (CNTs).[33]

For an electrically functioning paper device, the printable CNT electrodes must first be coated with a water-resistant dielectric parylene-C film, followed by a water-repellent hydrophobic Teflon AF 1600 film (see the Experimental Section), resulting in the cellulous fibers in the paper being confined solely because the substrate acts as a support for the multilayers in our current chip. **Figure** 1a shows schematics of the fabrication and the actuation of drops on a working paper chip by using an electrical power source attached to a programmable multiplex switching system. Our paper chip produced precise and controlled drop motions. In this paper, we present the fabrication of the APOC, suggest a few prototypes for patterned electrodes, and demonstrate comprehensive discrete fluidic manipulation of these electrodes. Our results show that the microfluidic chips can be used without significant modification in complex bioassay applications requiring immobilization of targeted antigens.[34] We successfully demonstrate that our prototype APOCs will ultimately be able to compete with conventional microfluidic devices in the near future, thereby enabling true point-of-care production and diagnostic activities (see Figure 1).

First, we describe the fundamental operating principles of this paper-based APOC. The driving force for the motion of the target drop can be understood in terms of electrowetting phenomenon, i.e., applying an electrostatic potential between a liquid drop and a counter-electrode beneath the surface causes a static sessile drop in contact with a hydrophobic surface to spread or deform. Two different types of electrowetting fluidic systems have been developed thus far:[27] the first is a closed configuration in which drops are confined between two contacting plates, and the cover plate acts as a common grounded electrode with a direct electrical connection to the target drop. The second system is an open configuration in which drops are exposed to air such that two neighboring electrodes act sequentially as a ground and an electric potential supplier.[26,28] For a paper-based fluidic system, however, the open type is the only viable option because general papers are naturally flexible and opaque. The open chip configuration does not require channel walls to confine the drops; therefore, the chip can be conveniently accessed, and reagents can be dispensed using a discrete sample pipette. After a deformable drop is partially positioned on both electrodes, it can move towards the energized electrode, i.e., the high potential electrode.[26,28]

Figure 2 shows an actuated 3-μL drop on a pre-patterned paper chip with square-shaped CNT electrodes driven by a 70-V

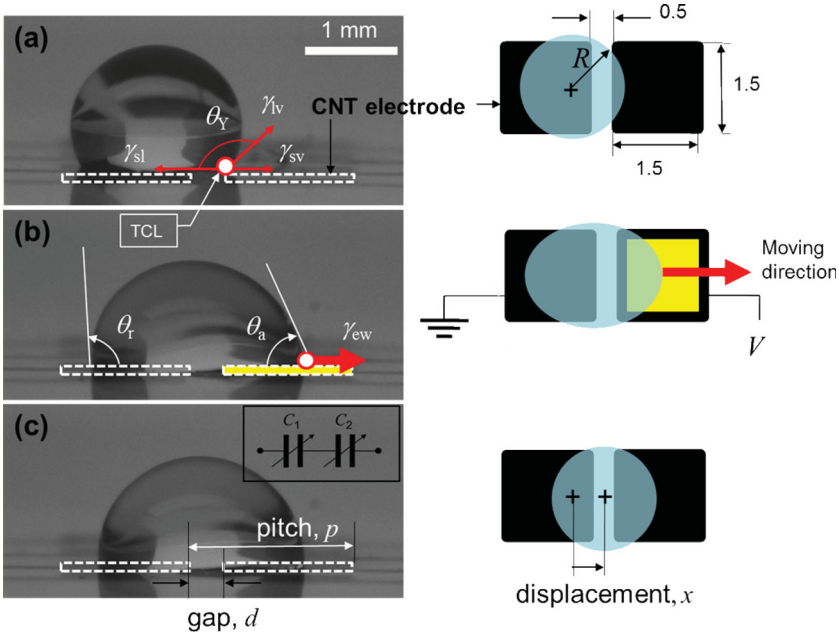

Figure 2. Drop actuation on an open, simple paper chip composed of two square electrodes, shown in photographic side views and schematic top views: a) digital sessile drop in its initial equilibrium state (unit: mm); b) deformed drop moving towards the energized electrode (yellow) under a DC voltage of 70 V; and c) drop stopped at its maximum displacement. Inset: the capacitors representing the equivalent electrostatic system consist of the drop and the chip.

DC voltage. Figure 2a shows that at zero voltage, the drop is in its equilibrium state, which satisfies Young's equilibrium condition for the triple contact line (TCL), i.e., the horizontal components of the interfacial tensions (γ) for vapor (v), liquid water (l), and solid substrate (s) phases satisfy the Young equation: $\gamma_{sv} = \gamma_{sl} + \gamma_{lv}\cos\theta_Y$, where θ_Y is Young's contact angle.[21,22,35] The Young–Lippmann equation for the contact angle (see Equation S3 in Section S1 of the Supporting Information) shows that an external voltage can cause a drop in either direct contact (as in a closed system) or indirect contact (as in an open system) with the high potential electrode to deform, depending on the electrowetting surface tension induced by the electric potential (yellow), γ_{ew}, acting opposite to γ_{sl} along the TCL (Figure 2b). Consequently, the deformed drop, which typically exhibits two different advancing and receding contact angles, θ_a and θ_r, in opposite directions owing to the distorted equipotential distribution of the electric field, slides on the fresh dielectric surface towards the energized electrode (Figure 2c) because of the Laplace pressure resulting from the net electrowetting force acting in the direction of motion which is proportional to the difference of contact angles, $|\cos\theta_r - \cos\theta_a|$, according to Furmidge's model.[22,32,35,36] Note that there is an alternative eletromechanical formalism for the electrowetting force, yet it is equivalent to the above thermodynamical approach.[21,28] Thus, when a series of conducting patterns is printed in the form of a rail, sequentially energizing each pattern causes the drop to translate linearly along the electrode rail.[26–28,35]

In comparison to a closed system, which needs at least one directly connected electrode, a drop in an open system must always simultaneously overlap the two neighboring electrodes along the rail before and after actuation because the electrowetting actuation force is significantly lower than that of closed system (Figure 2a).[28,35] The chip is then essentially equivalent to two capacitors composed of two planar electrodes that are connected in series via a deformable conductive drop, assuming that the liquid drop is a perfect conductor (see the inset to Figure 2c). Cooney et al.[37] showed theoretically that the force acting on the drop vanishes near the midpoint between the electrodes, indicating that the midway is a stable equilibrium position corresponding to the minimum electrostatic potential energy of two serially connected variable capacitors, C_1 and C_2. Herein, the electrowetting-induced surface tension is given by $\gamma_{ew} = C_{eq}V^2/2$, where C_{eq} denotes the equivalent capacitance of C_1 and C_2. Consequently, drop can be stopped inadvertently between the electrodes, when the moving drop does not have enough acceleration by γ_{ew} against the strong frictional force .[32,35] Abdelgawad, Park, and Wheeler[28] suggested that this undesirable termination in the motion can be prevented by tuning the major optimization parameters of the system, i.e., by i) reducing the gap distance, ii) varying the patterning motif of the electrodes, or iii) changing the type of electrical power and the type of its supply mode.

In our current fabrication scheme, the electrodes were printed on paper using an office inkjet printer in the overlaid printing mode to improve the conductivity of the CNT patterns such that the reduction in the size of the gap between electrodes (Figure 2c) was inherently restricted to approximately 100 μm.[33] For this reason, we must determine the optimized pitch (p) for a given gap (d) and drop volume with a base radius (R) to increase the drop displacement, such that the drop could be flawlessly actuated along a rail consisting of three electrodes (see Figures S1a–g in the Supporting Information). For example, for a given base diameter of a drop on the surface, $\phi = 2R$, the following relative geometric criterion for a drop on an array of electrodes must be satisfied: $\phi > p + d$. In this case, a single drop overlaps three electrodes simultaneously (see Figure S1a, Supporting Information, and the corresponding schematics), which is a required condition for continuous drop actuation when the power switched to the next pair of electrodes. We found a simpler way of satisfying the aforementioned geometric criterion by introducing an asymmetrically patterned rail of electrodes with convex and concave motifs on two sides of a square (i.e., the method mentioned in item (ii) above (see Figure S2 in the Supporting Information); however, the drop could be not be reliably actuated up to the third electrode for the square-patterned electrode rail system. This result was obtained because the drop displacement was not sufficient to satisfy another kinetic criterion required for the continuous actuation of the drop; i.e., the displacement must exceed the pitch of the electrode rail: $x > p$, (see Figure S1d, Supporting Information, and the corresponding schematic).

A simple way to increase the displacement is to increase the electrical power. **Figure 3**a shows that increasing the DC voltage from 70 to 120 V improved the average displacement. Imperfections in the drop motion and intermittent stops were minimized using two additional methods for improving the continuity of the actuation: i) reduction of the surface friction, and ii) changing from DC to AC voltage. The enhanced kinetic features of the drop motion were quantified by studying the displacement (x) of a 10-μL actuated drop as a function of the gap size (d) between two half-infinite planar electrodes. Figure 3a–c shows the measured displacements for a) an uncoated Teflon surface, b) an oil-coated surface for two selected DC voltages, and c) an oil-coated surface for three selected AC voltages.[37–41] First, comparing (a) with (b) clearly shows that oil coating increases the average displacements to 1.4 mm and 0.8 mm for DC voltages of 70 and 120 V, respectively; next, comparing (b) with (c) shows that applying an AC voltage instead of a DC voltage further increases the displacements by approximately 1.0 mm for the two cases on the oil-coated surface. Expressing the degree of extension as a relative ratio of the displacement to the pitch, $\kappa = x/p$, where p is given by 2.0 mm as an example (the green cross marker in the figures), produces a dimensionless factor to indicate whether the kinetic criterion for actuation is satisfied. Figure 3b shows that oil lubrication resulted in dimensionless degrees of extension of 0.9 and 1.1 for DC voltages of 70 and 120 V, respectively, and changing to an AC voltage increased the displacements to 1.4 and 1.6 for AC voltages of 70 and 120 V_{rms} (Figure 3c), respectively. The chip could not be actuated for an uncoated surface under the condition $\kappa << 1$. With the oil-coated surface, the chip could be actuated, but not reliably, at the two selected DC voltages because $\kappa \approx 1$ (Figure 3b). However, the chip could be reliably actuated for the two selected AC voltages at 70 and 120 V_{rms} because $\kappa > 1$ (Figure 3c). The lowest working voltages were estimated by measuring the displacement versus the gap size: the lowest AC voltage for the chip in this configuration was 40 V_{rms}.[42] These experimental results showed that an AC driving voltage,

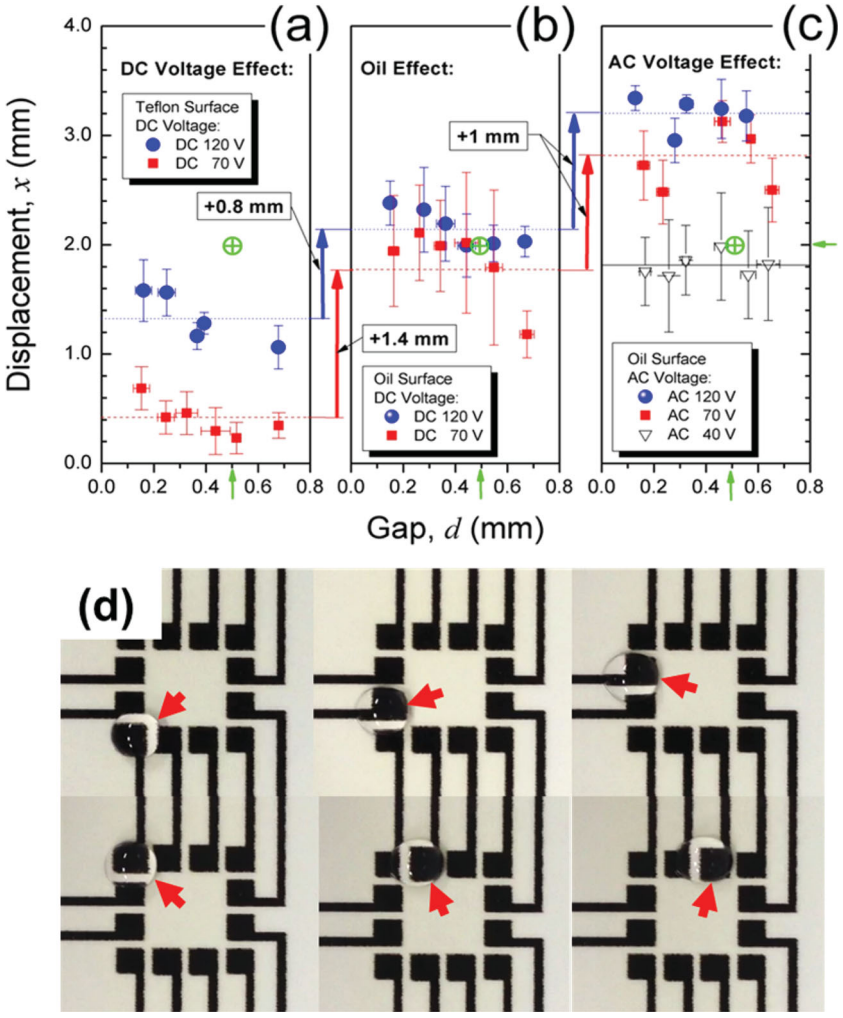

Figure 3. Drop displacement as a function of the gap size for different surface conditions and different magnitudes and types of driving voltages: a) uncoated Teflon surface, b) oil-coated surface driven by two DC voltages of 70 V and 120 V, and c) oil-coated surface driven by three AC driving voltages of 40 V_{rms}, 70 V_{rms}, and 120 V_{rms} with a low fixed frequency of 1 kHz. The black solid line, the red dashed line, and the blue line indicate the average displacements at 40 V, 70 V, and 120 V, respectively. d) Continuous drop motion on an oil-coated paper chip with a patterned rail of symmetric square-electrodes with a pitch and gap of 1.5 mm and 0.5 mm, respectively; the required minimum displacements of 2 mm for a gap of 0.5 mm are marked with green plus signs in graphs of (a–c). It shows excellent and reliable drop actuation under a 70 V_{rms} (see Video S1, Supporting Information).

coupled with an oil coating, acted as a reliable and efficient source for continuous drop actuation (see Figure 3d and Video S1, Supporting Information, for a square-patterned 70 V_{rms} electrode system) because the total displacement was increased sufficiently to satisfy the kinetic criterion for all of the types of paper chips studied.

To increase the volume of the target drops, we further tested printed electrodes with a stripe rail shape, as was first suggested by Washizu in 1998.[26] **Figure 4** shows snapshots from the continuous actuations for a paper chip composed of a stripe pattern with a 1.3-mm pitch, a 0.4-mm gap and a relatively large length that was coated with silicone oil. The following operational actuations were carried out: a) three stationary 8-μL drops were initially deposited on the chip; b) the second drop moved along the rail of stripe electrodes; c) the second drop merged with the third stationary drop via a perfect inelastic collision; d) the merged drop (which was double the volume of each of the initial drops) moved in the retro direction; e) the merged drop combined with the first drop, tripling its volume relative to the initial drop volume; and f–g) the merged drop moved back and forth. Figures 4h–j show that the same processes resulted in the 40th merged drop merging digitally with a stationary drop pre-positioned on the left-most side, and the 41st merged drop moving to the right-most electrode, corresponding to a total volume of 328 μL. We were then able to perform a satisfactory back-and-forth translational motion with the final merged drop (see Video S2, Supporting Information). The drops moved very smoothly during all of the manipulations described above. We further obtained the average speeds of drop movements, ranged from 0.1 cm s^{-1} to 3.5 cm s^{-1}, depending on the volume of drops and the applied voltages. (see Figure S3 in the Supporting Information). The stripe patterns were sufficiently long that whenever the drops merged, we did not have to carefully increase the length of the electrode in proportional to the increased drop size in order to provide the maximum base area to supply the electrostatic energy. This consideration is important because instead of focusing on designing a pattern of electrodes that enables the sample drops to be properly actuated, we can manipulate the sample drops on an actual prototype paper chip and focus on the real applications of the chip.[21,28] Consequently, the chip design takes on an operational universality that can be applied to any device without consideration of the final product's target volume.

Finally, we fabricated a prototype APOC chip with stripe electrode patterns and two simple reactors. We tailored the pitch, gap, and length to 1.5 mm, 0.5 mm, and 4.0 mm, respectively. **Figure 5** shows the two reactors, each of which was in the vicinity of each of the two Y-shaped junctions that were used to implement the volumetric mixing process of the two reacting chemical reagents. We applied an AC voltage of 70 V_{rms} to transport three colored drops along a short-length rail, subsequently mixed the drops at each of the two Y junctions, and then actuated the merged drop along a long, transporting rail. During all of the actuations, the drop moved very smoothly, accurately, and reproducibly as programmed, corresponding to a high reliability for this chip system (see Video S3, Supporting Information). We emphasize that this APOC can be used directly as a bioassay device or for a scheduled volumetric mixing process, for which a product with a detectable colorimetric reaction is provided, as

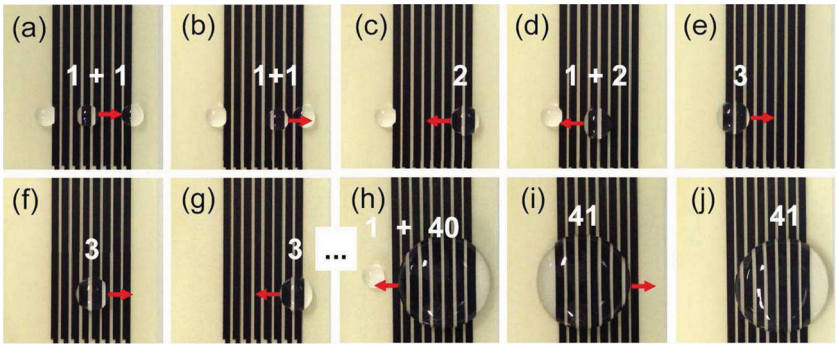

Figure 4. Bi-directional translation, actuation and merging of drops via collisions on an oil-coated paper chip composed of a rail of stripe-patterned CNT electrodes. The integer numbers represent the digital summation of the merging drops (see Video S2, Supporting Information).

shown in Figure 5c g. Similarly simple, but applicable, optically detectable reactions can be found in numerous research reports, especially reports in the field of bioassay devices for healthcare diagnosis.[5,9,12] To further improve our current APOC, we may motorize the syringe dispensing, thereby effectively implementing sequential volumetric mixing for the liquid reagents: i.e., our APOC would be fully equipped with all of the operational functions of an active LOC.

In summary, active, paper-based, microfluidic chips driven by electrowetting were fabricated. Instead of using the passive capillary force on the pulp in the paper to actuate a continuous flow of a liquid sample, we used inkjet printed electrodes to transport a single, discrete drop or a group of digital liquid drops perfectly along programmed trajectories. The patterned electrodes, which were designed on a desktop computer, were printed on paper with conductive CNT ink by using an office inkjet printer. This simple design and fabrication process can save time and significantly reduce costs. We found that tuning the surface tension by using lubricating silicone oil and an AC driving voltage at a low frequency was critical to overcoming the technical obstacles posed by low printing resolution and enabled various lab-on-chip operations, such as transporting, merging and mixing, to be realized for a prototype APOC chip, in particular an APOC chip with a stripe electrode pattern. These techniques of using paper-based chips with simple inkjet printing can certainly be extended to develop various active devices, such as paper batteries,[7,43] electric paper,[14] and various bioassays

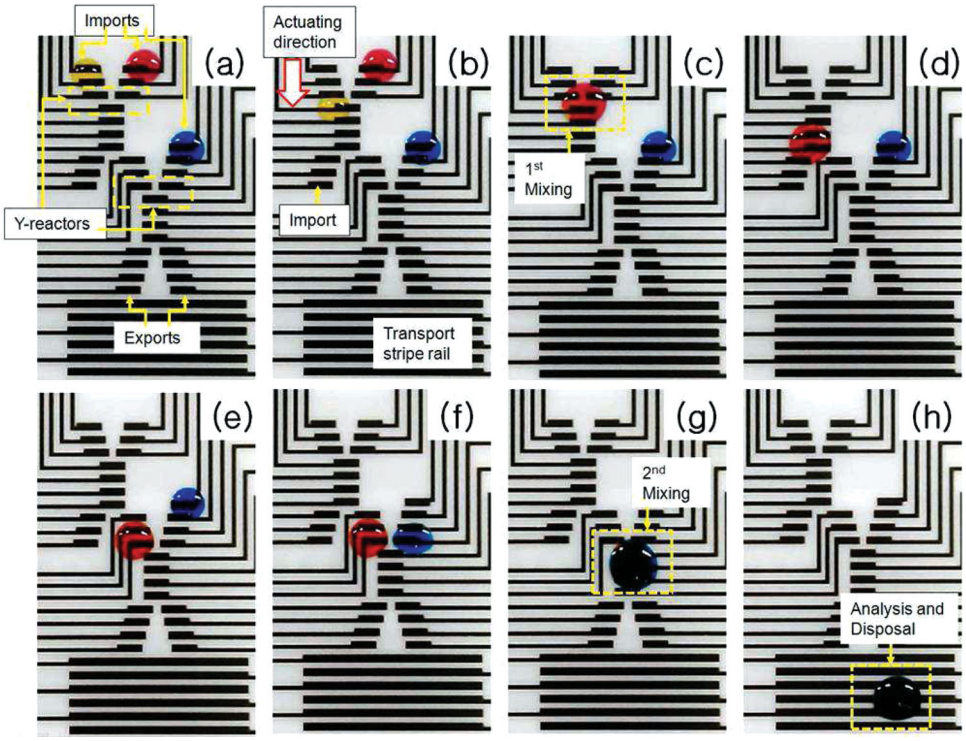

Figure 5. Prototype of a digital microfluidic paper chip composed of a stripe-patterned rail of electrodes with the novel functionalities of chemical reactors, showing active and efficient mixing of three drops. This superior performance implies that the prototype can be used directly to analyze chemical reactions for mixed analytes and reagents. Description of operations: a–c) a yellow and a red drop move separately and mix at the first Y junction; d–g) the merged drop moves and mixes with a blue drop at the second Y junction; and h) a drop with triple the volume of the other drops moves to the disposal rail (see Video S3, Supporting Information).

(e.g., for MALDI and ELISA devices),[12,29,30] based on flexible, disposable, and conductive paper substrates.

Experimental Section

Inkjet Printing a CNT Film: Aqueous, conductive CNT ink was formulated for use with an inkjet printer. The average length of the CNTs, purchased from TCI America Co. (Portland, USA), was 1 μm, which was sufficient to prevent blockage of the fine nozzle (orifice diameter of 20-μm) of the inkjet printer. To homogenize the CNT ink well, we added a non-ionic surfactant with a naphthyl group and used kinetic ball milling. The details of CNT ink fabrication are described in Kwon et al.[33] The CNT ink was printed on photo paper by using an office inkjet printer (model: EPSON Stylus T10), and the array of electrodes was designed using Adobe Flash graphic software. The surfaces and the cross-sections of the photo paper were examined using atomic force microscopy and scanning electron microscopy (Figure S4 in the Supporting Information) to confirm the quality of the printed CNT electrodes, which were sufficiently homogeneous to be highly conductive.[33]

Depositing Functional Films for APOC: To make active, paper-based microfluidic chips driven by an electrowetting-induced surface tension, we coated the printed electrodes with two functional films, a hydrophobic, amorphous Teflon film (AF 1600, DuPont, 200-nm thick) and a dielectric parylene-C film (Sigma-Aldrich, 1-μm thick), by using spin-coating and chemical vapor deposition, respectively. The samples were then baked at 170 °C for 30 minutes. A 3-μL drop of silicone oil (Sigma-Aldrich) with a kinetic viscosity of 10 cSt was spin-coated at 2000 rpm for 30 s onto a paper chip with an estimated thickness of approximately 500 nm. The oil was a siloxane polymer with organic CH_3 side chains and was used as a lubricant and to adjust the surface tension of the paper chips.

Electric System for Drop Actuation: Keithley 2400 and 2702 units were used as the electric power source and the multiflex relay, respectively, for switching the power to the each electrode printed on the paper.

Supporting Information

Supporting Information is available from the Wiley Online Library or from the author.

Acknowledgements

This work was supported by the Nuclear Research R&D Program, the Mid-career Researcher Program (2011–0017539), the Advanced Research Center for Nuclear Excellence and Basic Science Research Program (2013R1A1A2010265), Leading Foreign Research Institute Recruitment Program (2013K1A4A3055268), through the National Research Foundation of Korea (NRF) funded by the Ministry of Science, ICT & Future Planning (MSIP), Korea.

Received: October 8, 2013
Published online: January 13, 2014

[1] J. P. Rolland, D. A. Mourey, *MRS Bulletin* **2013**, *38*, 299.
[2] D. Tobjxörk, R. Österbacka, *Adv. Mater.* **2011**, *23*, 1935.
[3] M. Alava, K. Niskanen, *Rep. Prog. Phys.* **2006**, *69*, 669.
[4] a)D. Klemm, B. Heublein, H.-P. Fink, A. Bohn, *Angew. Chem.* **2005**, *117*, 3422; b)*Angew. Chem. Int. Ed.* **2005**, *44*, 3358.
[5] G. Chitnis, Z. Ding, C.-L. Chang, C. A. Savran, B. Ziaie, *Lab Chip* **2011**, *11*, 1161.
[6] J. Kim, S. Yun, S. K. Mahadeva, K. Yun, S. Y. Yang, M. Maniruzzaman, *Sensors* **2010**, *10*, 1473.
[7] N. K. Thom, K. Yeung, M. B. Pillion, S. T. Phillips, *Lab Chip* **2012**, *12*, 1768.
[8] X. Li, D. R. Ballerini, W. Shen, *Biomicrofluidics* **2012**, *6*, 011301.
[9] L. Gervais, N. de Rooij, E. Delamarche, *Adv. Mater.* **2011**, *23*, H151.
[10] A. K. Yetisen, M. S. Akram, C. R. Lowe, *Lab Chip* **2013**, *13*, 2210.
[11] D. D. Liana, B. Raguse, J. J. Gooding, E. Chow, *Sensors* **2012**, *12*, 11505.
[12] A. Apilux, Y. Ukita, M. Chikae, O. Chailapakul, Y. Takamura, *Lab Chip* **2013**, *13*, 126.
[13] K. Abe, K. Suzuki, D. Citterio, *Anal. Chem.* **2008**, *80*, 6928.
[14] P. Andersson, D. Nilsson, P.-O. Svensson, M. Chen, A. Malmström, T. Remonen, T. Kugler, M. Berggren, *Adv. Mater.* **2002**, *14*, 1460.
[15] a)A. W. Martinez, S. T. Phillips, M. J. Butte, G. M. Whitesides, *Angew. Chem.* **2007**, *119*, 1340; b) *Angew. Chem. Int. Ed. Engl.* **2007**, *46*, 1318.
[16] G. M. Whitesides, *Nature* **2006**, *442*, 368.
[17] A. W. Martinez, S. T. Phillips, Z. Nie, C.-M. Cheng, E. Carrilho, B. J. Wiley, G. M. Whitesides, *Lab Chip* **2010**, *10*, 2499.
[18] U. Zschieschang, T. Yamamoto, K. Takimiya, H. Kuwabara, M. Ikeda, T. Seitani, T. Someya, H. Klauk, *Adv. Mater.* **2011**, *23*, 654.
[19] M. C. Barr, J. A. Rowehl, R. R. Lunt, J. Xu, A. Wang, C. M. Boyce, S. G. Im, V. Bulović, K. Gleason, *Adv. Mater.* **2011**, *23*, 3500.
[20] Y. Zhang, T.-H. Wang, *Adv. Mater.* **2013**, *25*, 2903.
[21] F. Mugele, J.-C. Baret, *J. Phys. Condens. Mater.* **2005**, *17*, R705.
[22] W. C. Nelson, C.-J. Kim, *J. Adhesion Sci. Technol.* **2012**, *26*, 1747.
[23] M. G. Pollack, R. B. Fair, A. D. Shenderov, *Appl. Phys. Lett.* **2000**, *77*, 1725.
[24] R. B. Fair, *Microfluid. Nanofluid.* **2007**, *3*, 245.
[25] D. Mark, S. Haeberle, G. Roth, F. von Sterren, R. Zengerle, *Chem. Soc. Rev.* **2010**, *39*, 1153.
[26] M. Washizu, *IEEE Trans. Ind. Appl.* **1998**, *34*, 732.
[27] U.-C. Yi, C.-J. Kim, *J. Micromech. Microeng.* **2006**, *16*, 2053.
[28] M. Abdelgawad, P. Park, A. R. Wheeler, *J. Appl. Phys.* **2009**, *105*, 094506.
[29] D. Chatterjee, A. J. Ytterberg, S. U. Son, J. A. Loo, R. L. Garrell, *Anal. Chem.* **2010**, *82*, 2095.
[30] Z. Nie, F. Deiss, X. Liu, O. Akbulut, G. M. Whitesides, *Lab Chip* **2010**, *10*, 3163.
[31] H. Moon, S. K. Cho, R. L. Garrell, C.-J. Kim, *J. Appl. Phys.* **2002**, *92*, 4080.
[32] M. Abdelgawad, S. L. S. Ferire, H. Yang, A. R. Wheeler, *Lab Chip* **2008**, *8*, 672.
[33] O.-S. Kwon, H. Kim, H. Ko, J. Lee, B. Lee, C.-H. Jung, J.-H. Choi, K. Shin, *Carbon* **2013**, *58*, 116.
[34] E. Delamarche, D. Juncker, H. Schmid, *Adv. Mater.* **2005**, *17*, 2911.
[35] A. Torkkeli, Ph.D. Thesis, Helsinki University of Technology, Finland **2003**.
[36] C. G. L. Furmidge, *J. Colloid Sci.* **1962**, *17*, 309.
[37] C. G. Cooney, C.-Y. Chen, M. R. Emerling, A. Nadim, J. D. Sterling, *Microfluid. Nanofluid.* **2006**, *2*, 435.
[38] R. F. Rios, H. Dodiuk, S. Kenig, S. McCarthy, A. Dotan, *J. Adhesion Sci. Technol.* **2007**, *21*, 227.
[39] H. Ren, R. B. Fair, M. G. Pollack, E. J. Shaughnessy, *Sens. Actuators B* **2002**, *87*, 201.
[40] J. D. Smith, R. Dhiman, S. Anand, E. Reza-Garduno, R. E. Cohen, G. H. McKinley, K. K. Varanasi, *Soft Matter* **2013**, *9*, 1772.
[41] K. Zhou, J. Heikenfeld, K. A. Dean, E. M. Howard, M. R. Johnson, *J. Micromech. Microeng.* **2009**, *19*, 065029.
[42] J. Berthier, P. Dubois, P. Clementz, P. Claustre, C. Peponnet, Y. Fouillet, *Sens. Actuators A* **2007**, *134*, 471.
[43] L. Hu, J. W. Choi, Y. Yang, S. Jeong, F. L. Mantia, L.-F. Cui, Y. Cui, *Proc. Natl. Acad. Sci. USA* **2009**, *106*, 21490.